Electronic Supplementary Material (ESI) for New Journal of Chemistry.

Supporting Information

Triazole-Amide isosteric pyridine-based supramolecular gelators in metal ion and biothiol sensing with excellent performance in adsorption of heavy metal ions and picric acid from water

Atanu Panja and Kumaresh Ghosh*

Department of Chemistry, University of Kalyani, Kalyani-741235, India.
Email: ghosh_k2003@yahoo.co.in;kumareshchem18@klyuniv.ac.in

Table of contents

Table S1. Results of gelation test for **1-4**.

Solvent	1	2	3	4
DMSO	S	S	S	S
DMF	S	S	S	S
THF	S	PS	S	S
CH_3CN	S	PS	S	S
CH_3OH	S	PS	S	I
$CHCl_3$	S	PS	S	PS
$CHCl_3$: CH_3OH (1:1, v/v)	S	S	S	S
Diethyl ether	I	I	I	I
Hexane	I	I	I	I
Petroleum ether	I	I	I	I
DCM	S	PS	S	PS
DMSO: H_2O (1:1, v/v)	G	G	PG	S
DMSO: H_2O (1:2, v/v)	G (2 mg/mL)	G (7 mg/mL)	G (10 mg/mL)	S
DMF: H_2O (1:1, v/v)	S	S	S	S
THF: H_2O (1:1, v/v)	S	P	S	S
CH_3CN: H_2O (1:1, v/v)	P	P	P	S
CH_3OH: H_2O (1:1, v/v)	P	P	P	P
DMSO: H_2O + Ag^+ (1:2, v/v)	-	-	-	G (2 mg/mL)
DMF: H_2O + Ag^+ (1:2, v/v)	-	-	-	G

S = Solution; G = Gel (mgc); I = Insoluble; P = Precipitation. Gelation tests were carried out by taking 10 mg of respective compounds in 1 ml of respective solvents.

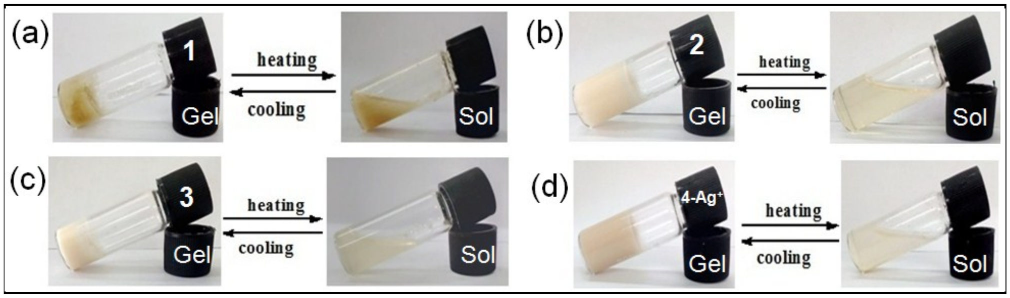

Fig. S1. Pictorial representation of the thermo reversibility of the DMSO: H_2O (1:2, v/v) gel of (a) **1**, (b) **2**, (c) **3** and (d) Ag-gel of **4**.

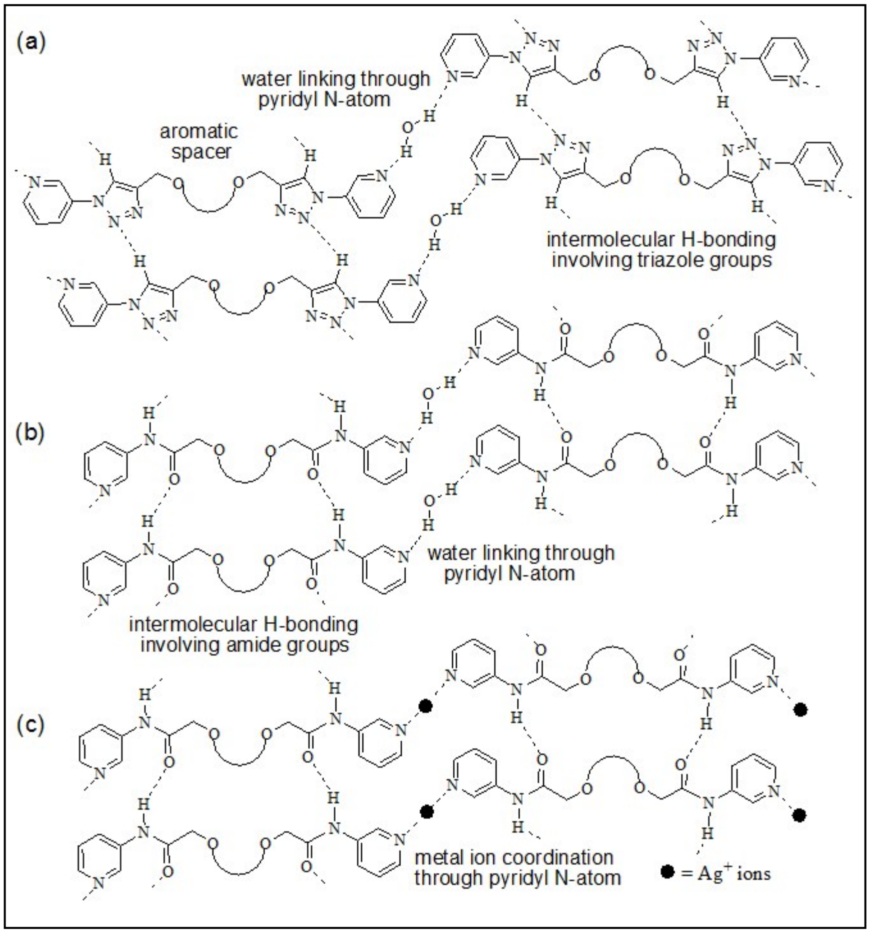

Fig. S2. Probable binding modes of (a) **1** and **3**, (b) **2** and (c) **4** in gel state.

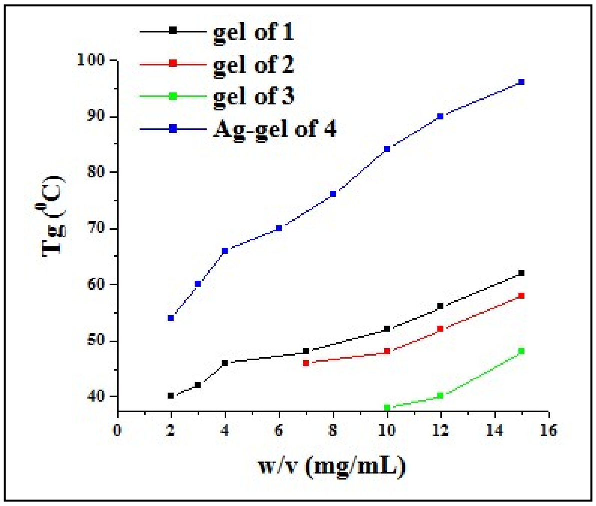

Fig. S3. Variation of gel melting temperature (T_g) with increase in concentration of gelators.

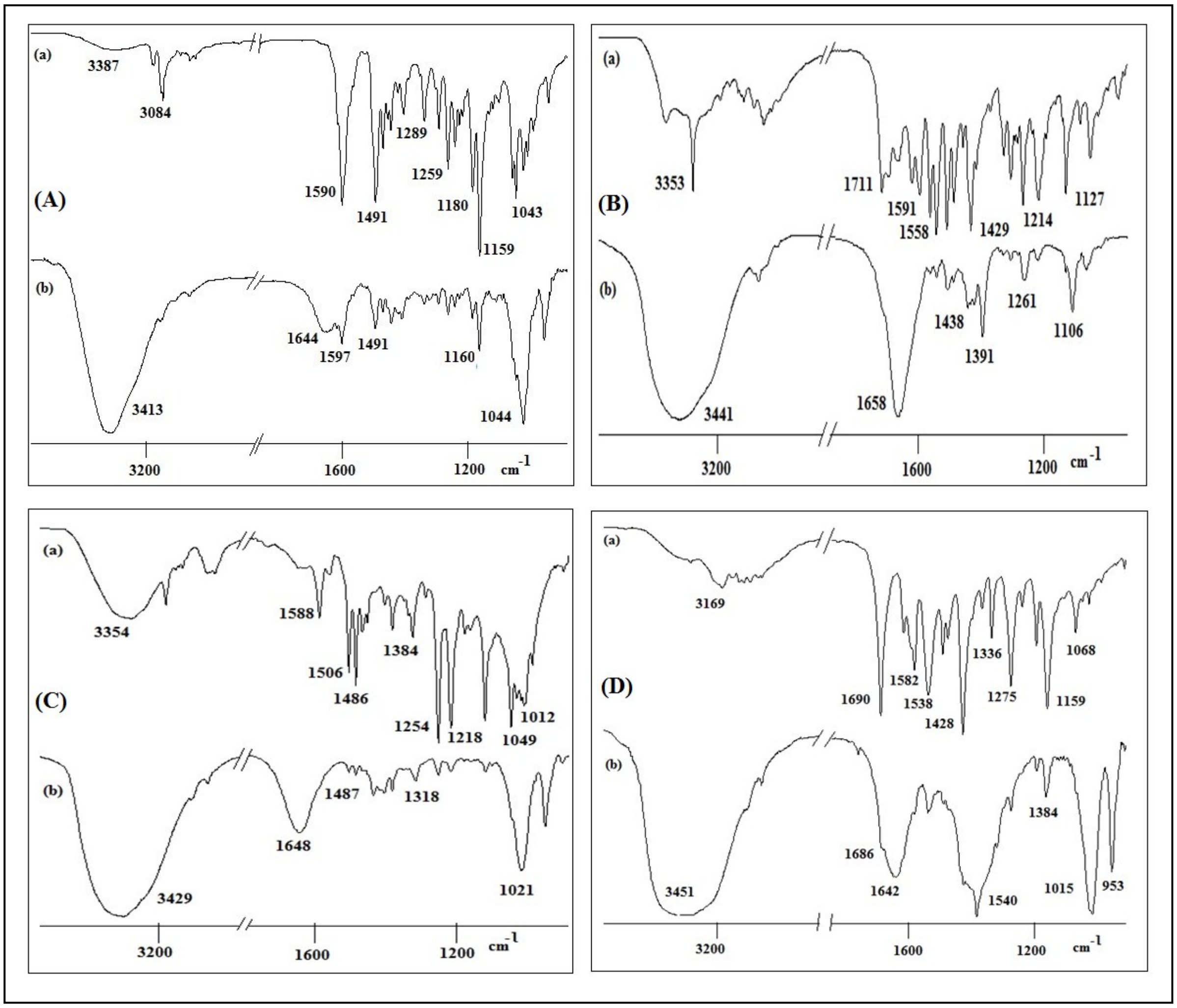

Fig. S4. Partial FTIR spectra of (A) **1**, (B) **2**, (C) **3** and (D) **4** in (a) amorphous and (b) gel state, respectively.

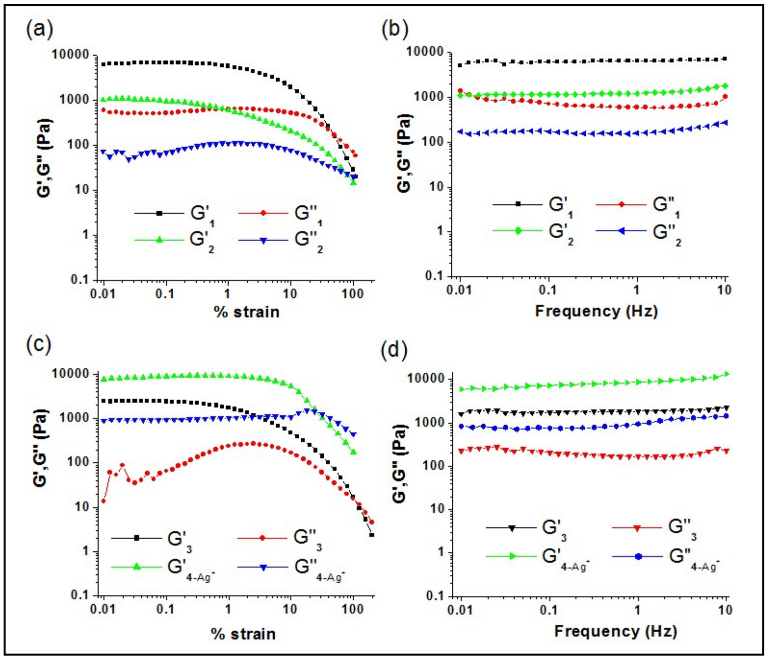

Compound (2 x mgc)/mL	Strain at crossover (%)	G'_{av} (Pa)	G''_{av} (Pa)	tan δ (G''_{av}/ G'_{av})
1	46	6233	733	0.12
2	74	1240	175	0.14
3	106	1852	206	0.11
4-Ag$^+$	26	8253	946	0.11

Fig. S5. Rheology study of the gels of **1**-**3** and **4**-Ag$^+$ gel obtained from DMSO/H$_2$O (1:2, v/v); (a) and (c) amplitude sweep and (b) and (d) frequency sweep experiments. All the gels were prepared at a concentration double of respective mgc of the gels.

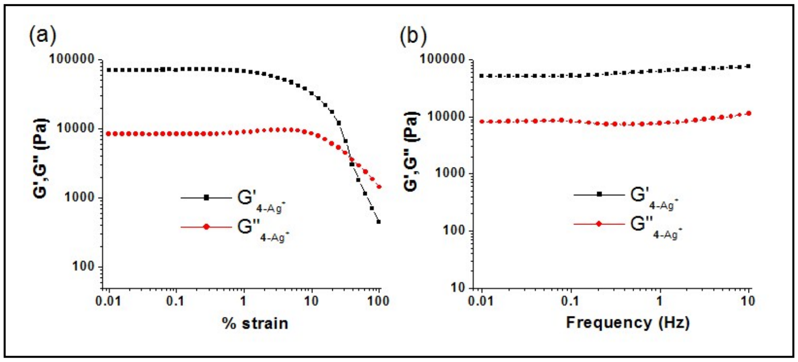

Compound (10 mg/mL)	Strain at crossover (%)	G'_{av} (Pa)	G''_{av} (Pa)	tan δ (G''_{av}/ G'_{av})
4-Ag^+	37	54955	7970	0.14

Fig. S6. Rheology study of the Ag^+-gel of **4** (10 mg/mL) obtained from DMSO/H_2O (1:2, v/v); (a) and (c) amplitude sweep and (b) and (d) frequency sweep experiments.

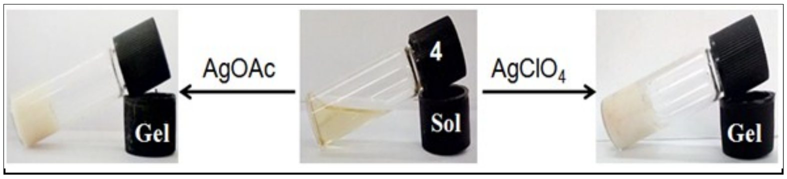

Fig. S7. Photograph showing the preparation of gels from **4** in presence of AgOAc and $AgClO_4$.

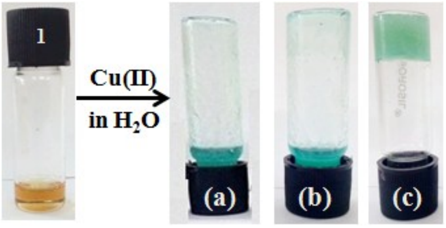

Gelator	Metal ion	Entry	Conc. (M)	Equiv.	status
1 (2 mg in 0.33 mL DMSO)	Cu^{2+} (0.66 mL in H_2O)	(a)	5 x 10^{-2}	7.0	Sol
		(b)	2 x 10^{-2}	2.8	Sol
		(c)	1 x 10^{-2}	1.4	Gel

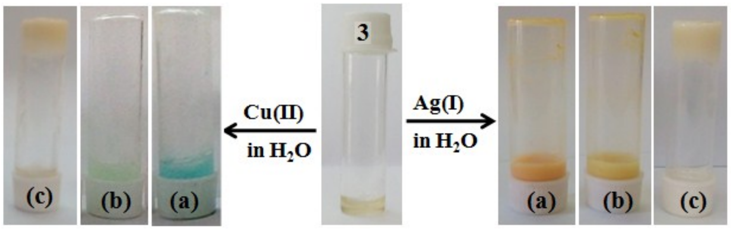

Gelator	Metal ion	Entry	Conc. (M)	Equiv.	status	Metal ion	Entry	Conc. (M)	Equiv.	status
3 (10 mg in 0.33 mL DMSO)	Cu^{2+} (0.66 mL in H_2O)	(a)	5 x 10^{-2}	1.4	Sol	Ag^{+} (0.66 mL in H_2O)	(a)	5 x 10^{-2}	1.4	Sol
		(b)	8 x 10^{-3}	0.2	Sol		(b)	5 x 10^{-3}	0.14	Sol
		(c)	5 x 10^{-3}	0.14	Gel		(c)	2 x 10^{-3}	0.06	Gel

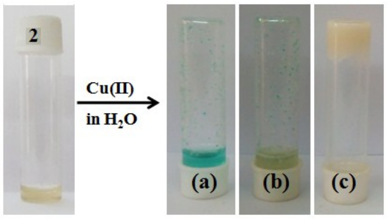

Gelator	Metal ion	Entry	Conc. (M)	Equiv.	status
2 (7 mg in 0.33 mL DMSO)	Cu^{2+} (0.66 mL in H_2O)	(a)	5 x 10^{-2}	1.7	Sol
		(b)	8 x 10^{-3}	0.3	Sol
		(c)	5 x 10^{-3}	0.18	Gel

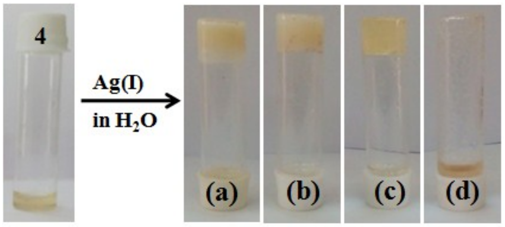

4 (mg/mL)	Ag^{+} ion equiv.	status
2	1	Gel
2	0.5	Sol
1	2	Gel
10	0.5	Gel
10	0.1	Gel

Gelator	Metal ion	Entry	Conc. (M)	Equiv.	status
4 (10 mg in 0.33 mL DMSO)	Ag^{+} (0.66 mL in H_2O)	(a)	5 x 10^{-2}	1.3	Gel
		(b)	8 x 10^{-3}	0.2	Gel
		(c)	5 x 10^{-3}	0.13	Gel
		(d)	2 x 10^{-3}	0.05	Sol

Fig. S8. Photographs and tables showing the sensitivity of the gelators **1-4** towards Cu^{2+} and Ag^{+} ions.

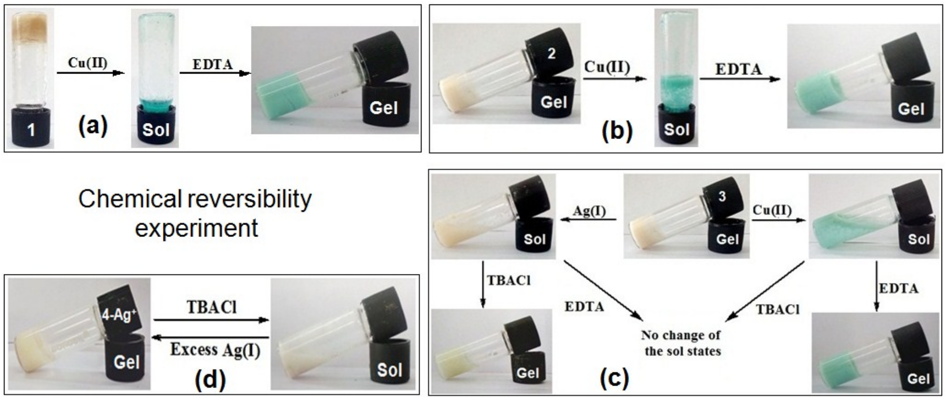

Fig. S9. Responsiveness of the gels of (a) **1**, (b) **2**, (c) **3** and (d) **4** in presence of different chemical analytes.

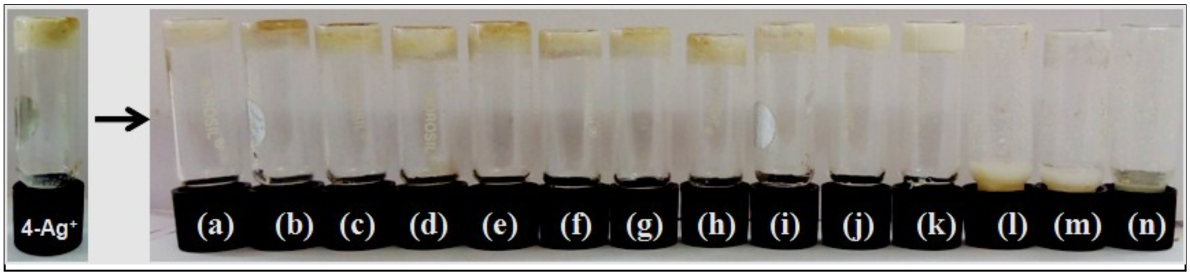

Fig. S10. Responsiveness of the **4**-Ag^+ gel (at mgc) toward different amino acids (2 equiv., $c = 0.05$ M) [a. glycine, b. L-valine, c. L-alanine, d. L-phenylalanine, e. L-proline, f. L-serine, g. L-lysine, h. L-threonine, i. L-hystidine, j. L-methionine, k. L-glutamic acid, l. L-cysteine, m. DL-homocysteine and n. L-glutathione; photograph was taken after 1h].

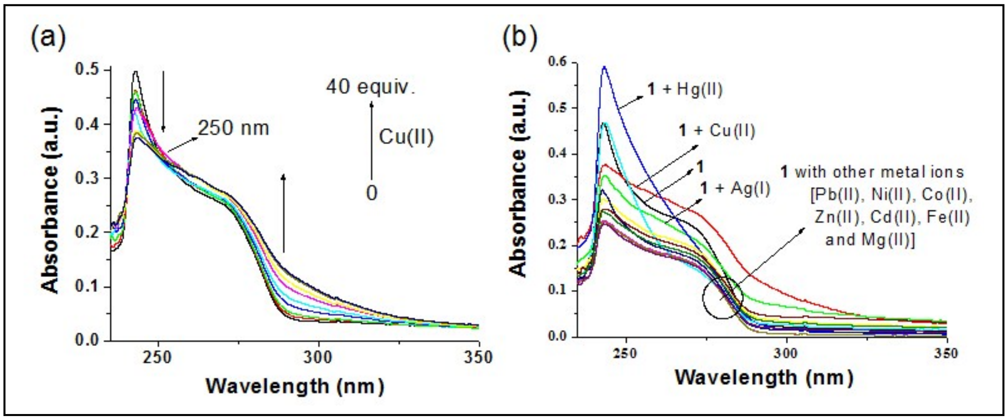

Fig. S11. Change in absorbance of **1** ($c = 2.50 \times 10^{-5}$ M) upon addition of 40 equiv. amounts of (a) Cu^{2+} and (b) different metal ions (as perchlorate salts, $c = 1.0 \times 10^{-3}$ M) in DMSO/H_2O (1:2, v/v).

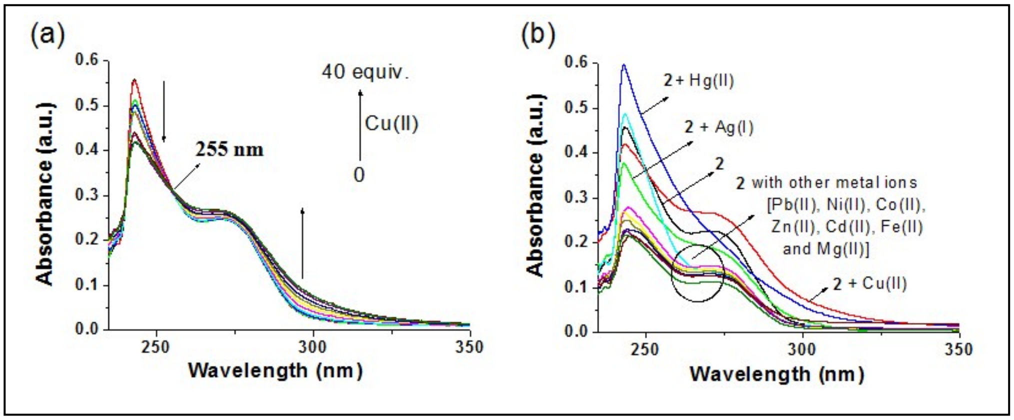

Fig. S12. Change in absorbance of **2** (*c* = 2.50 x 10^{-5} M) upon addition of 40 equiv. amounts of (a) Cu^{2+} and (b) different metal ions (as perchlorate salts, *c* = 1.0 x 10^{-3} M) in DMSO/H_2O (1:2, v/v).

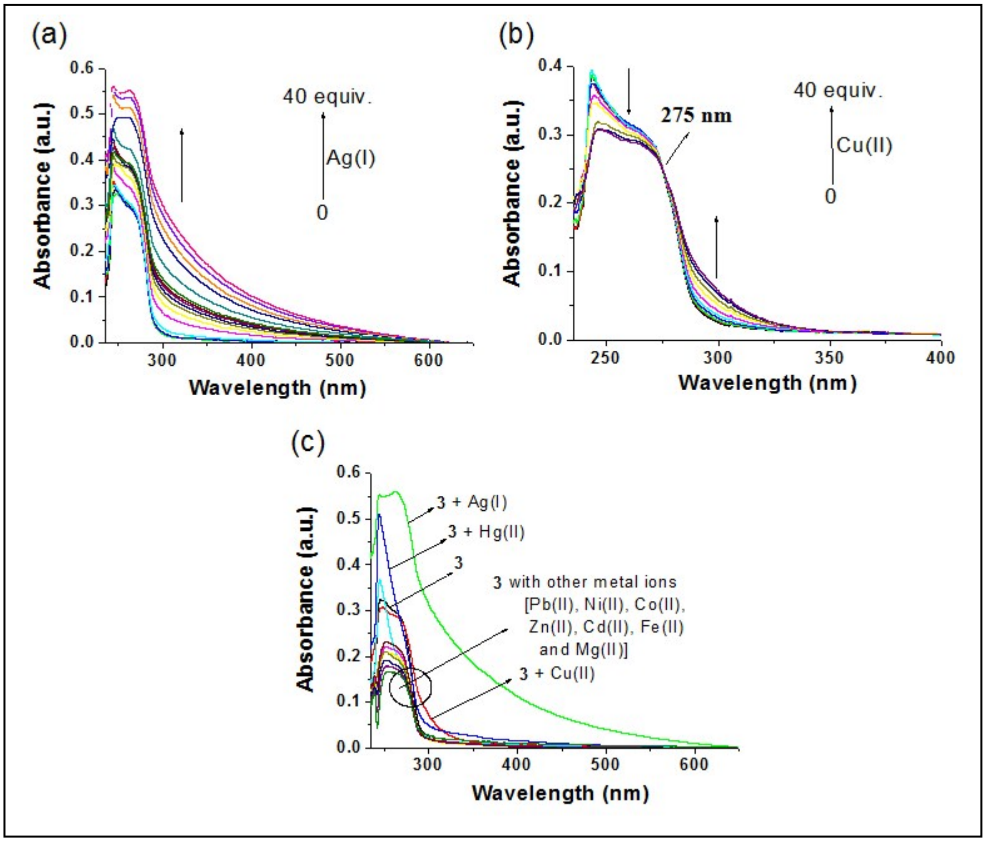

Fig. S13. Change in absorbance of **3** (*c* = 2.50 x 10^{-5} M) upon addition of 40 equiv. amounts of (a) Ag^{+}, (b) Cu^{2+} and (c) different metal ions (*c* = 1.0 x 10^{-3} M) in DMSO: H_2O (1:2, v/v).

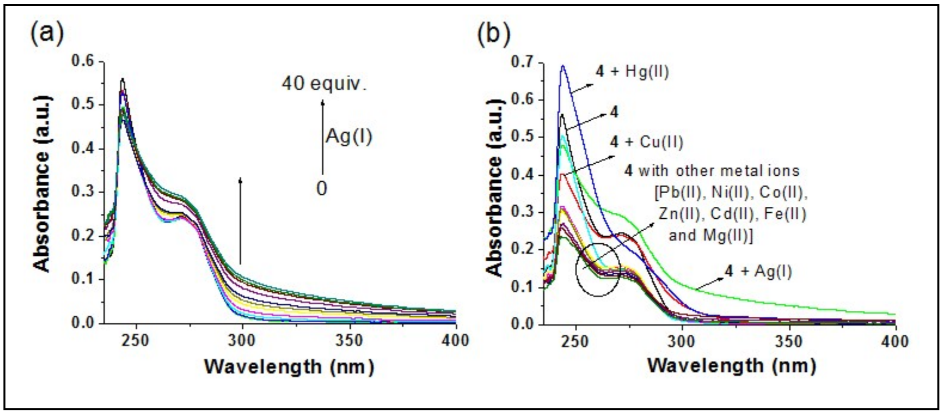

Fig. S14. Change in absorbance of **4** (c = 2.50 x 10^{-5} M) upon addition of 40 equiv. amounts of (a) Ag^+ and (b) different metal ions (c = 1.0 x 10^{-3} M) in DMSO: H_2O (1:2, v/v).

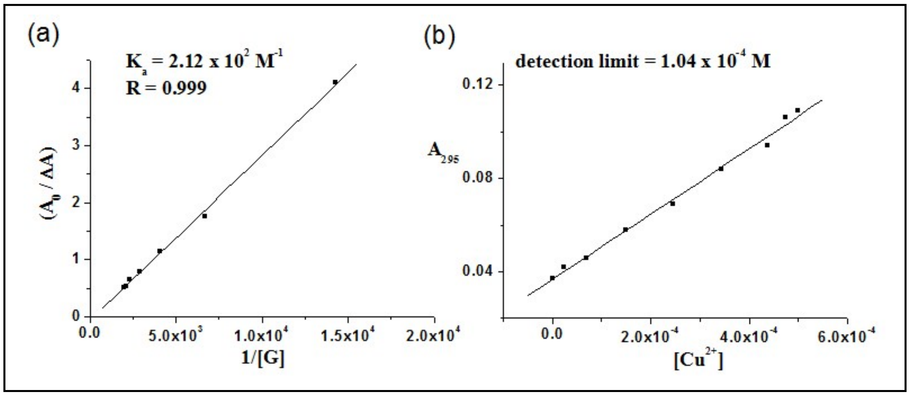

Fig. S15. (a) Benesi–Hilderband plot and (b) detection limit of **1** (c = 2.5 x 10^{-5} M) for Cu^{2+} ion at 295 nm (c = 1.0 x 10^{-3} M) in DMSO: H_2O (1:2, v/v) from UV-vis titration.

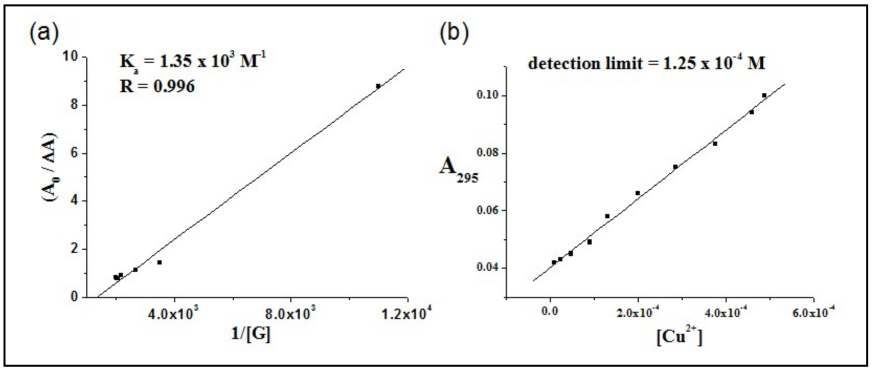

Fig. S16. (a) Benesi–Hilderband plot and (b) detection limit of **2** (c = 2.5 x 10^{-5} M) for Cu^{2+} ion at 295 nm (c = 1.0 x 10^{-3} M) in DMSO: H_2O (1:2, v/v) from UV-vis titration.

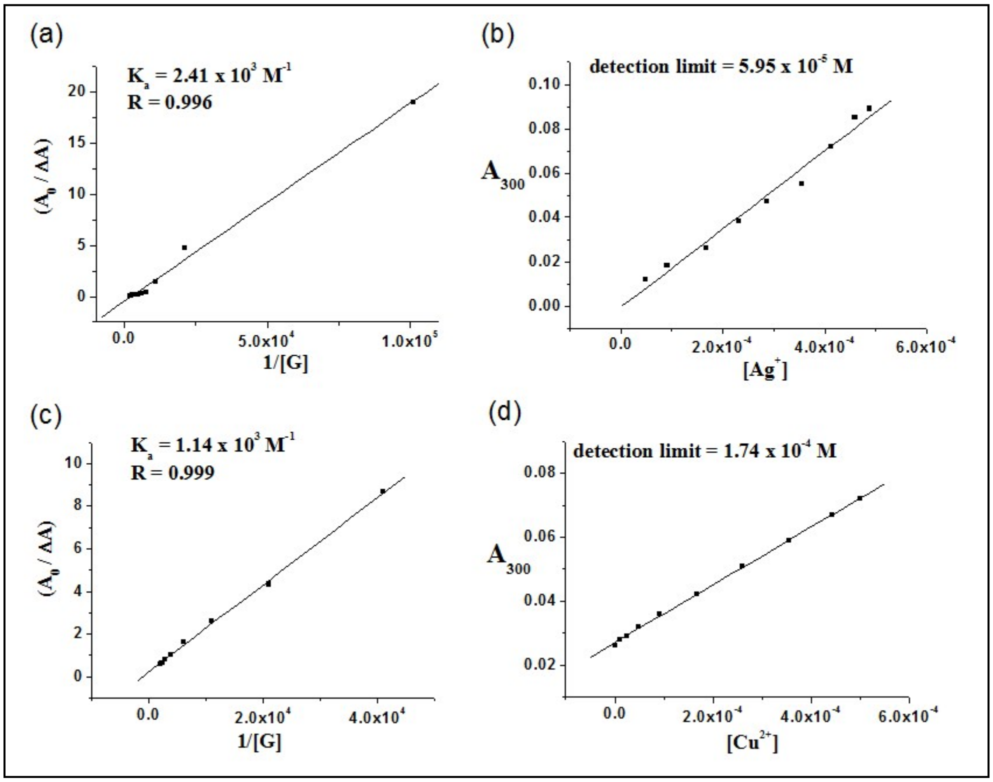

Fig. S17. Benesi–Hilderband plot (a and c) detection limit (b and d) of **3** (*c* = 2.5 x 10^{-5} M) for Ag^+ and Cu^{2+} ions, respectively, at 300 nm (*c* = 1.0 x 10^{-3} M) in DMSO: H_2O (1:2, v/v) from UV-vis titration.

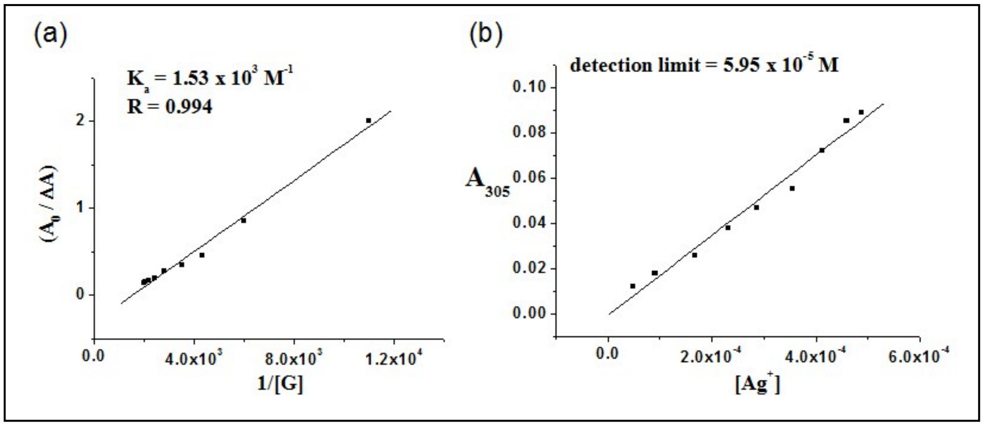

Fig. S18. (a) Benesi–Hilderband plot and (b) detection limit of **4** (*c* = 2.5 x 10^{-5} M) for Ag^+ ion at 305 nm (*c* = 1.0 x 10^{-3} M) in DMSO: H_2O (1:2, v/v) from UV-vis titration.

Table S2. Binding constants and detection limit values for the metal-ligand complexes.

Metal- ligand complex	Binding constant values (M^{-1}) From UV-vis titration	Detection limit values (M) From UV-vis titration
1 – Cu^{2+}	K = 2.12 x 10^2	1.04 x 10^{-4}
2 – Cu^{2+}	K = 1.35 x 10^3	1.25 x 10^{-4}
3 – Cu^{2+}	K = 1.14 x 10^3	1.74 x 10^{-4}
3 – Ag^+	K = 2.41 x 10^3	2.99 x 10^{-5}
4 – Ag^+	K = 1.53 x 10^3	5.95 x 10^{-5}

Metal ion binding analysis of compound 4 as representative example

Stock solution of the compound **4** (c = 2.50 x 10^{-5} M) was prepared in DMSO-H_2O (1:2, v/v). Stock solutions of different metal ions (taken as perchlorate salts) were also prepared in DMSO-H_2O (1:2, v/v) in the concentration of 1.0 x 10^{-3} M. Then 2 mL solution of compound **4** was taken in the cuvette and to the solution different metal ions were separately added in increasing amount (upto 40 equiv.). Upon gradual addition of different metal ions, the changes in absorbance of compound **4** were recorded. The absorbance values, concentrations of compound **4** and $AgClO_4$ (as an example) were used for determination of binding constant values as shown in Fig. S18.

Binding constant determination[1]

Benesi-Hildebrand plot was adopted to determine the binding constant value using the expression: $A_0/(A-A_0) = [\varepsilon_M/(\varepsilon_M - \varepsilon_C)](K_a^{-1}C_g^{-1} + 1)$, where ε_M and ε_C represent molar extinction coefficients for the gelator and the complex, respectively, at a selected wavelength, A_0 denotes the absorbance of free gelator at that specific wavelength and C_g is the concentration of the metal ions. The measured absorbance $A_0/(A-A_0)$ as a function of inverse of the metal ion concentration fits a linear relationship, indicating 1:1 stoichiometry of the gelator-metal ion complex. The ratio of the intercept to the slope was used to determine the binding constant K_a. Plots are shown in Figs. S15-S18.

Calculation of detection limit[2]

Detection limit was calculated using the UV-vis titration data. The absorbance of each compound was measured 5 times, and the standard deviation of blank measurement was achieved. To have the slope, absorbance values were plotted against concentrations of analyte. The detection limits were calculated using the equation: Detection limit = $3\sigma/k$, where σ is the standard deviation of blank measurement, and k is the slope. Plots are shown in Figs. S15-S18.

^{1}H NMR study

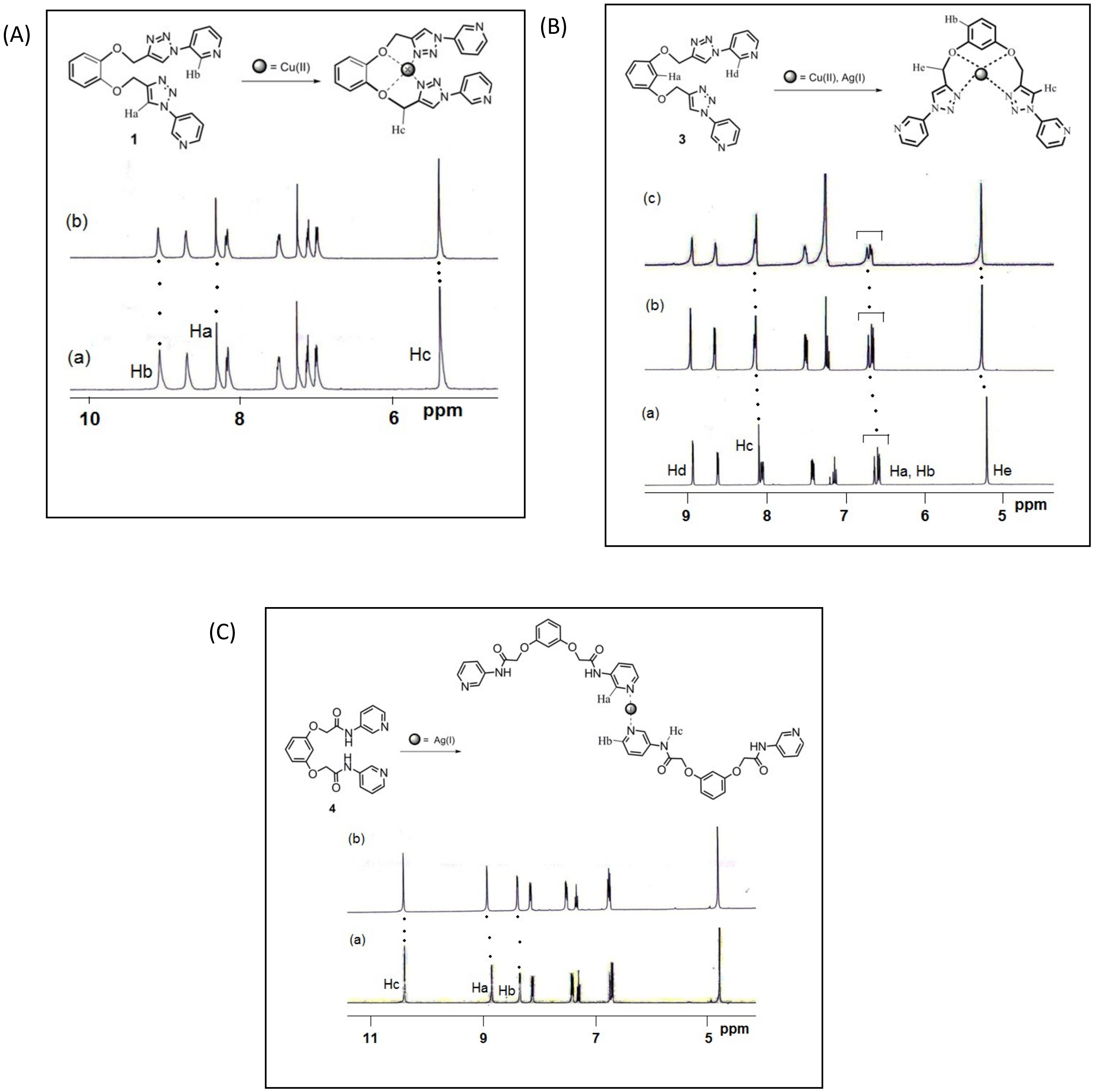

Fig. S19. (A) Comparison of ^{1}H NMR spectra of (a) **1** and (b) **1** with 1 equiv. of Cu^{2+} in $CDCl_3$. (B) Comparison of ^{1}H NMR spectra of (a) **3**, (b) **3** with 1 equiv. of Cu^{2+} and (c) **3** with 1 equiv. of Ag^+ in $CDCl_3$. (C) Comparison of ^{1}H NMR spectra of (a) **4** and (b) **4** with 1 equiv. of Ag^+ *d_6*-DMSO.

Table S3. Summary of thermal stability of the gels of **1**-**4** in presence of different metal salts.

Gelator	T_{gel} (°C) (± 2°C)	Doped metal salts	T_{gel} (°C) (± 2°C)	Gelator	T_{gel} (°C) (± 2°C)	Doped metal salts	T_{gel} (°C) (± 2°C)
1 (4 mg/mL)	46	$CoCl_2$	42	**2** (14 mg/mL)	56	$CoCl_2$	62
		$Ni(ClO_4)_2$	40			$Ni(ClO_4)_2$	62
		$Fe(ClO_4)_2$	38			$Fe(ClO_4)_2$	60
3 (20 mg/mL)	60	$CoCl_2$	54	**4** (4 mg/mL)	66	$CoCl_2$	76
		$Ni(ClO_4)_2$	52			$Ni(ClO_4)_2$	74
		$Fe(ClO_4)_2$	56			$Fe(ClO_4)_2$	72
						$Cu(ClO_4)_2$	72

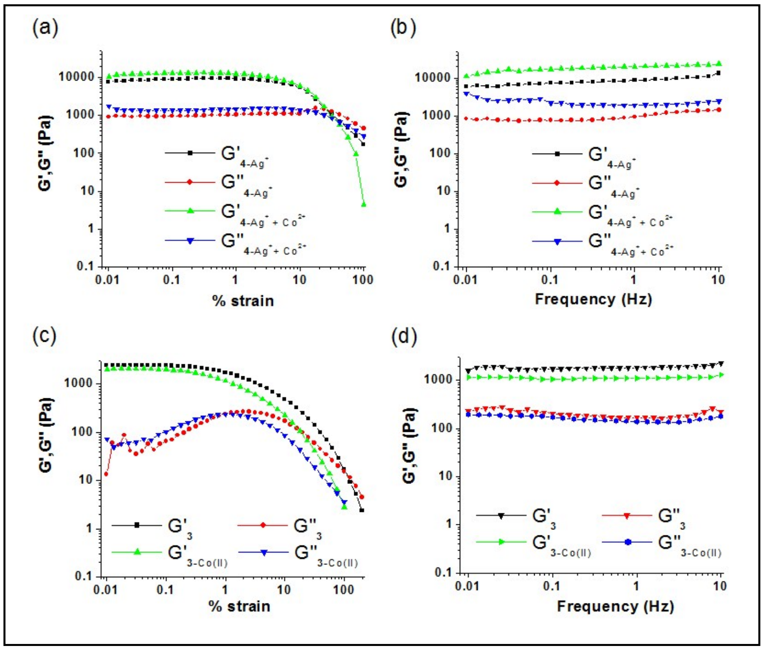

Compound (2 x mgc)/mL	Strain at crossover (%)	G'_{av} (Pa)	G''_{av} (Pa)	tan δ (G''_{av}/ G'_{av})
3	106	1852	206	0.11
$CoCl_2$-doped gel **3**	85	1135	162	0.14
4-Ag^+	26	8253	946	0.11
$CoCl_2$-doped **4**-Ag^+ gel	35	18478	233	0.13

Fig. S20. Rheology study of the $CoCl_2$-doped gel of **3** and **4**-Ag^+ gel; (a) and (c) amplitude sweep and (b) and (d) frequency sweep experiments.

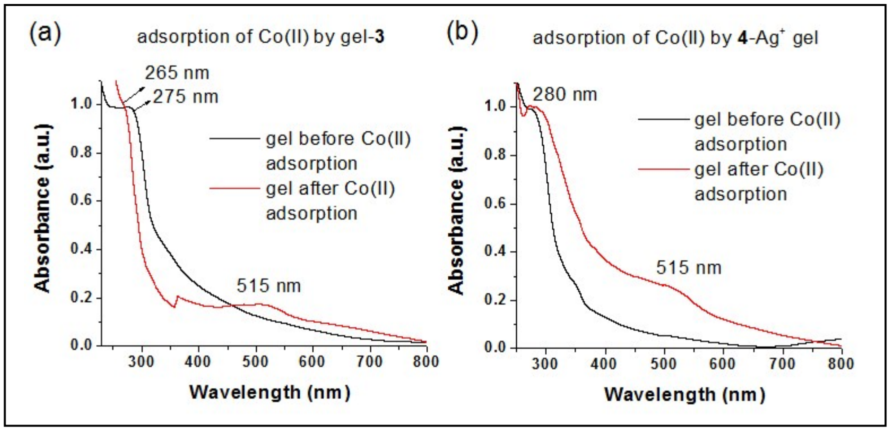

Fig. S21. Comparision of normalized UV-vis spectra of the gels of (a) **3** and (b) **4**-Ag$^+$ gel before and after $CoCl_2$-adsorption.

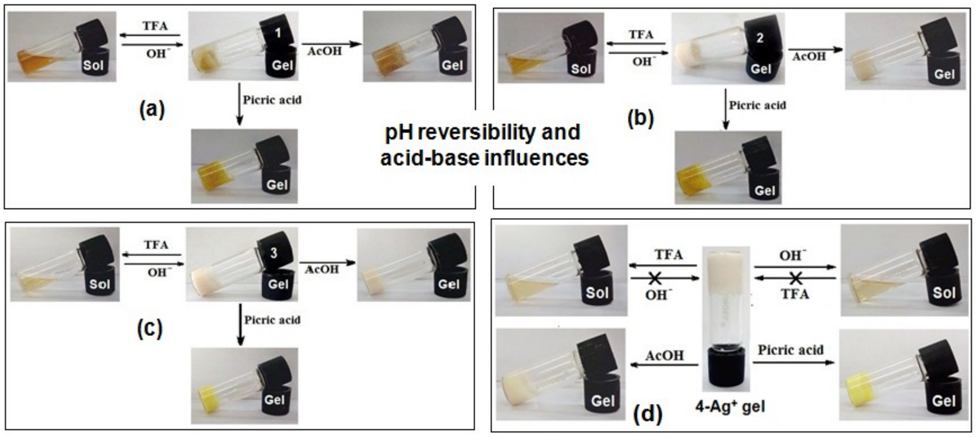

Fig. S22. Responsiveness of the gels of (a) **1**, (b) **2**, (c) **3** and (d) **4** in presence of different chemical analytes

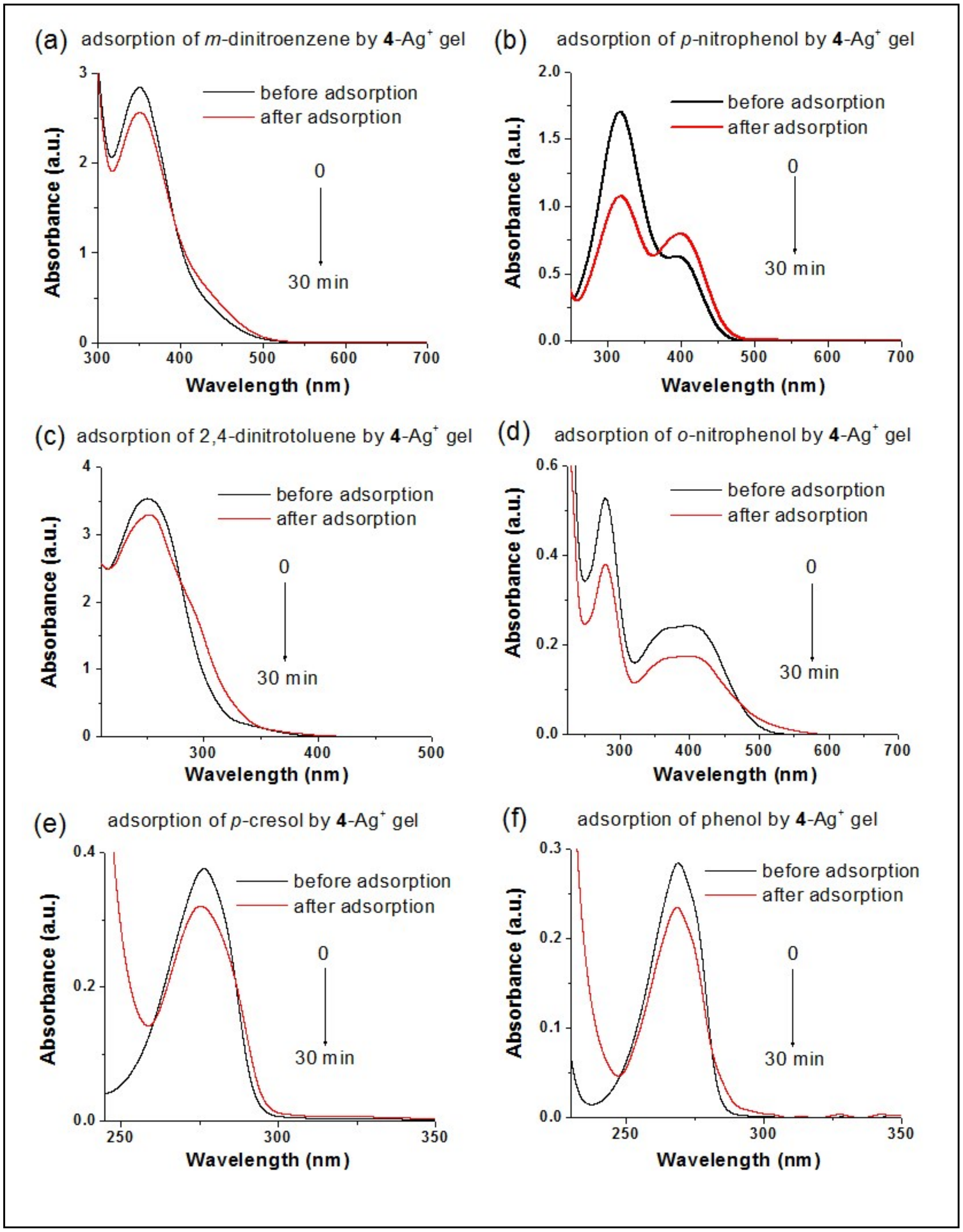

Fig. S23. Change in absorbance of (a) *m*-dinitrobenzene, (b) *p*-nitrophenol, (c) 2,4-dinitrotoluene, (d) *o*-nitrophenol, (e) *p*-cresol and (d) phenol during adsorption by **4**-Ag$^+$ gel [For *m*-dinitrobenzene, $c = 1 \times 10^{-4}$ M; for other cases, $c = 2 \times 10^{-4}$ M; for all the compounds, 3 mL of aqueous solution containing 0.01% CH_3CN was used for the experiment. For **4** (4 mg/mL), the gel was prepared with equiv. amount of $AgNO_3$].

Table S4. Summary of rheological properties of the **4**-Ag^+ gels before and after adsorption of PA (For **4**, the gel was prepared with 1 equiv. amount of $AgNO_3$).

Compound **4** (4 mg/mL)	Strain at crossover (%)	G'_{av} (Pa)	G''_{av} (Pa)	(G'_{av}/ $''_{av}$)	tan δ (G''_{av}/ G'_{av})
4-Ag^+	26	8253	946	8.72	0.11
PA- adsorbed **4**-Ag^+ gel	42	25497	3328	7.66	0.13

Table S5. Differential attributes of the isosteres.

Properties	**Triazole derivatives**	**Amide derivatives**
1. Gel properties i) Solvent (v/v) ii) mgc (mg/mL) in DMSO: H_2O (1:2) iii) T_{gel} (^oC) iv) Crossover point during amplitude sweep (% of strain)	Compound **1**. i) DMSO: H_2O (1:1 and 1:2) ii) 2 iii) 40 iv) 94 Compound **3**. i) DMSO: H_2O (1:2) ii) 10 iii) 38 iv) 116	Compound **2**. i) DMSO: H_2O (1:1 and 1:2) ii) 7 iii) 46 iv) 53 Compound **4**. i) DMSO: H_2O (1:2) in presence of Ag^+ ion ii) 2 iii) 54 iv) 38
2. Applications of the gels a) Metal ion responsiveness b) $CoCl_2$ adsorption (%) c) Picric acid adsorption (%)	Compound **1**. a) Cu^{2+} (weak sensitivity, metal induced gel-to-sol phase changes) b) 69 c) 55.10 Compound **3**. a) Cu^{2+} and Ag^+ (metal induced gel-to-sol phase change) b) 77 c) 49.18	Compound **2**. a) Cu^{2+} (high sensitivity, metal induced gel-to-sol phase changes) b) 43 c) 39.94 Compound **4**. a) Ag^+ (metal induced sol-to-gel phase change) b) 30.3 c) 90.79

Table S6: Comparison between present and previous observations.

Properties	**Triazole Derivatives (previous report)**[3]	**Amide derivatives (present report)**
1. Structure (Cholesteryl bistriazole *vs* pyridyl bistriazole)	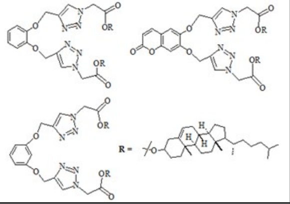	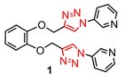 1 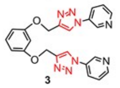 3
2. Gel forming solvent	**Catechol bistriazoles** $CHCl_3$: CH_3OH (1:1, v/v) **Resorcinol bistriazole** $CHCl_3$: CH_3OH (1:1, v/v)	**Catechol bistriazole 1** DMSO: H_2O (1:1 and 1:2) **Resorcinol bistriazole 3** DMSO: H_2O (1:2)
3. Metal ion responsiveness (metal induced gel-to-sol phase change)	**Catechol bistriazoles** Ag^+, Cu^{2+} and Hg^{2+} **Resorcinol bistriazole** Cu^{2+}	**Catechol bistriazole 1** Cu^{2+} **Resorcinol bistriazole 3** Ag^+ and Cu^{2+}

References

1. P. T. Chou, G. R. Wu, C. Y. Wei, C. C. Cheng, C. P. Chang and F. T. Hung, *J. Phys. Chem. B*, 2000, **104**, 7818.
2. A. R.Sarkar, C. H. Heo, M. Y. Park, H. W. Lee, H. M. Kim, *Chem. Commun.* **2014**, *50*, 1309.
3. K. Ghosh, A. Panja and S. Panja, *New. J. Chem*. 2016, **40**, 3476.

^{1}H NMR (CDCl$_3$, 400 MHz)

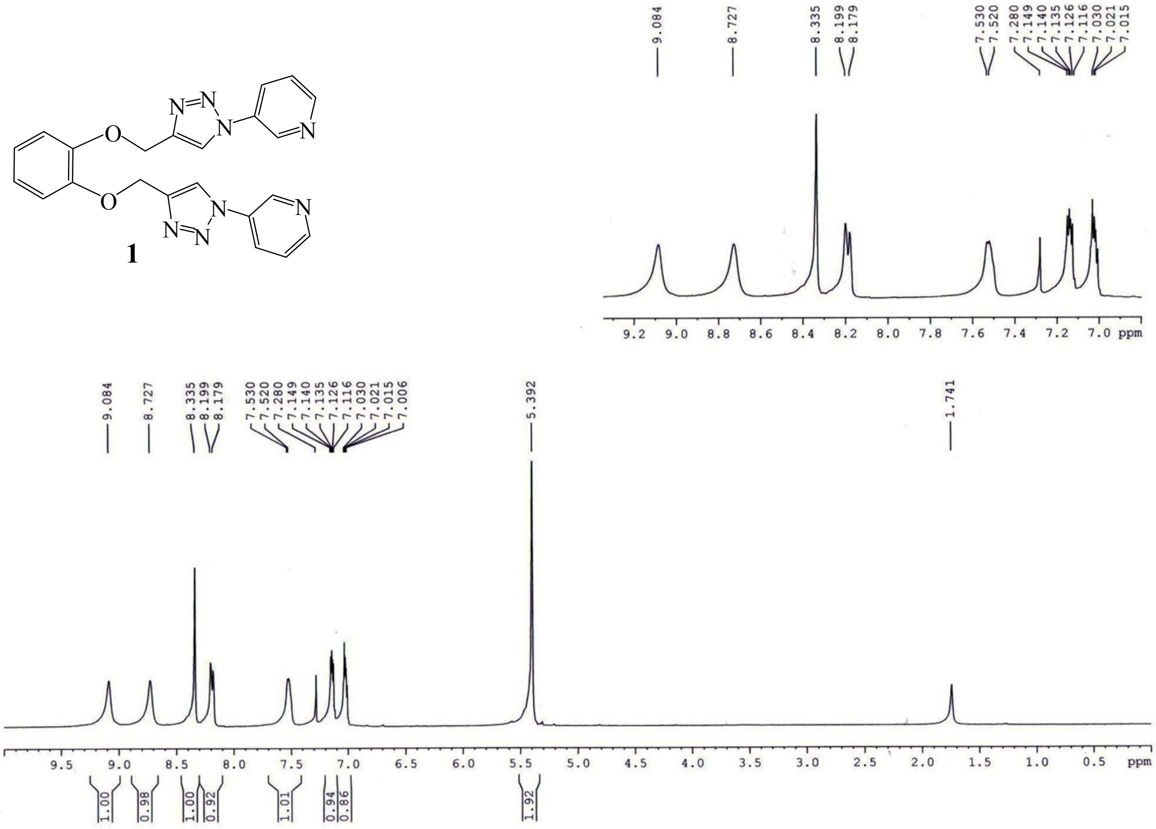

1

^{13}C NMR (CDCl$_3$, 100 MHz)

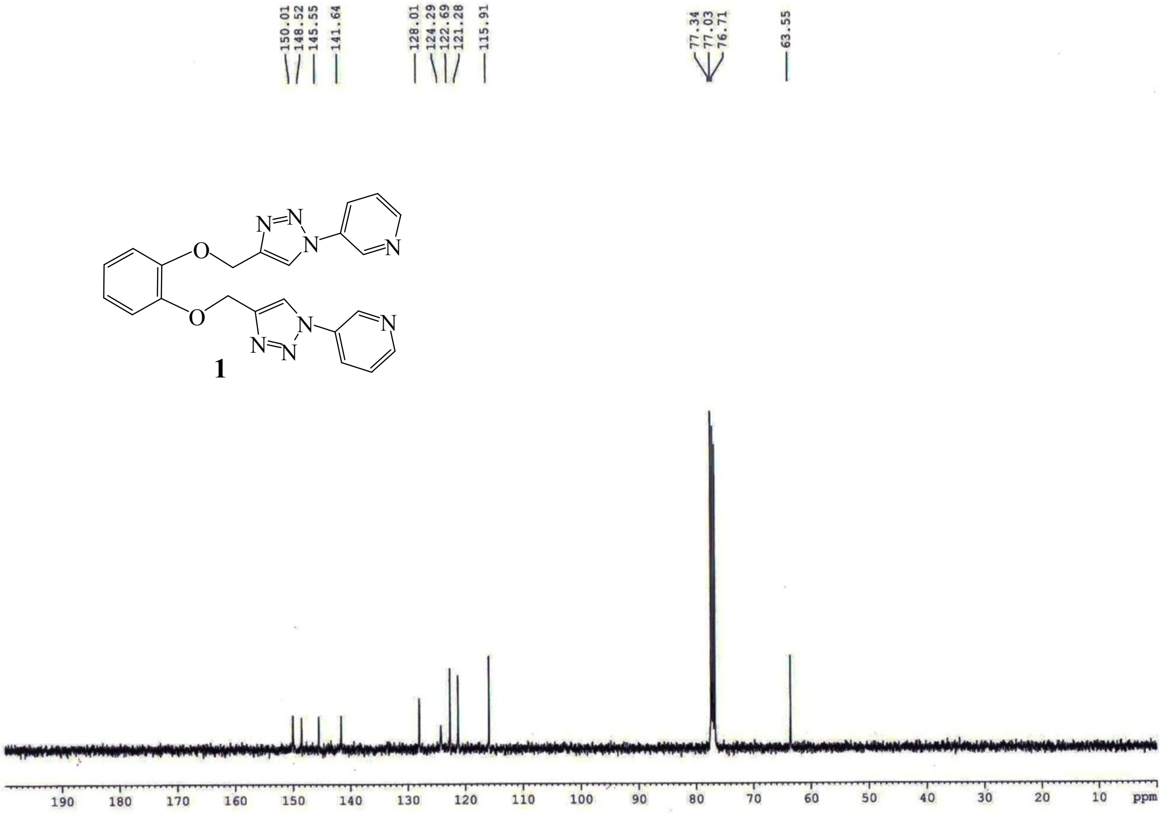

Mass spectrum of 1.

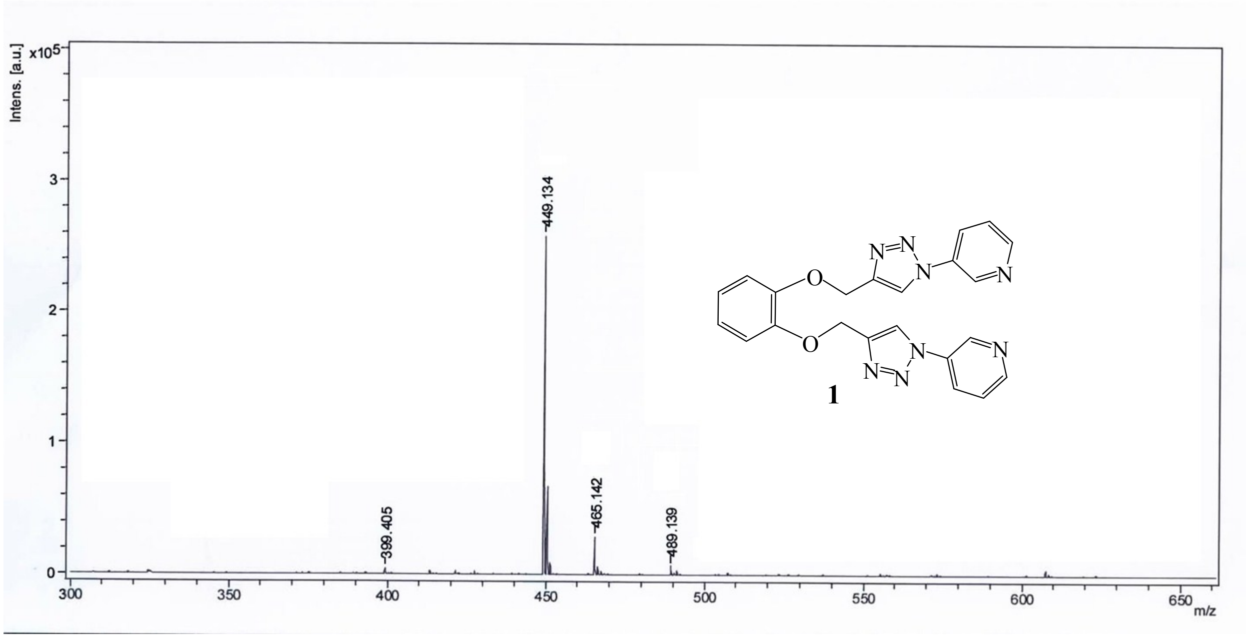

^{1}H NMR (d_6-DMSO, 400 MHz)

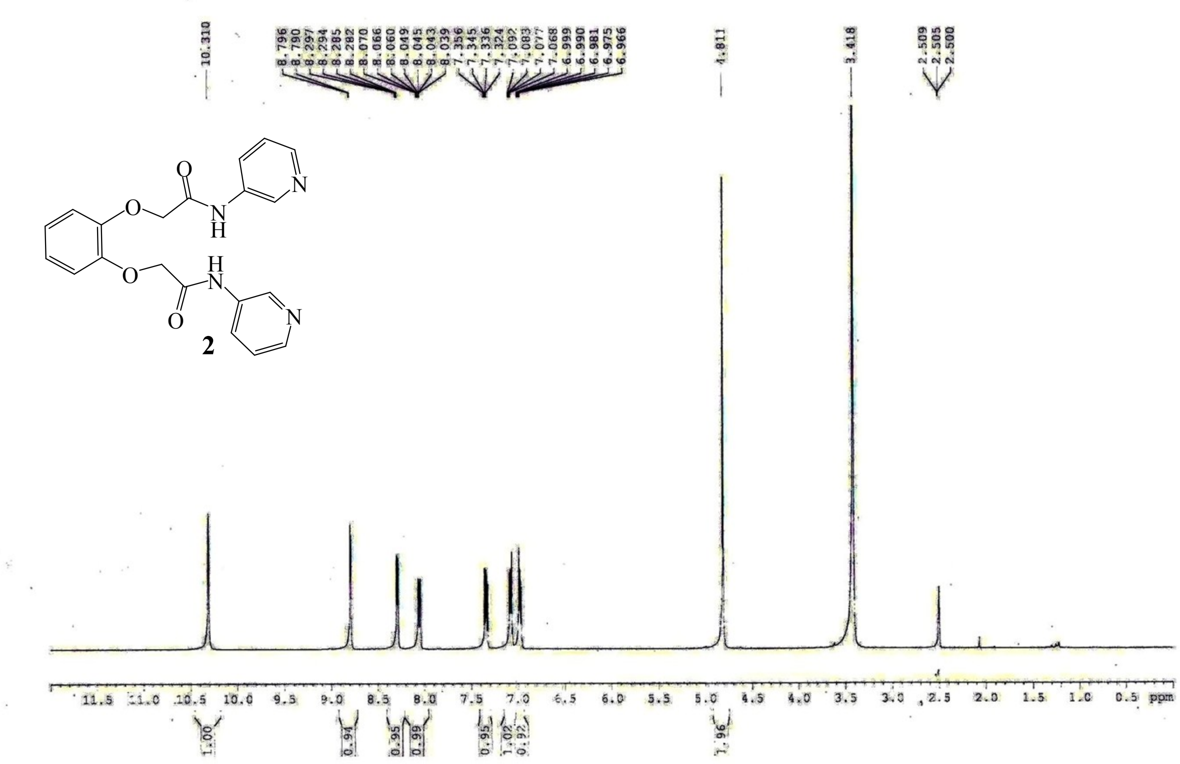

^{13}C NMR (d_6-DMSO, 100 MHz)

Mass spectrum of 2.

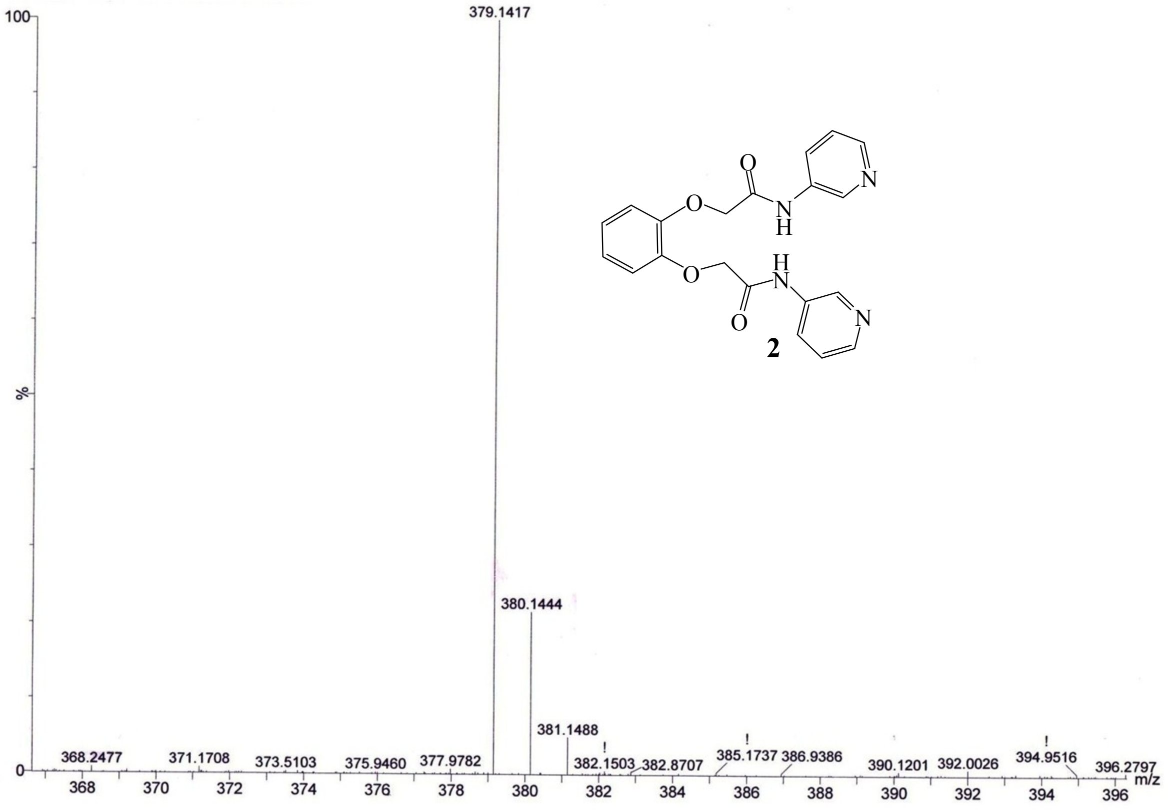

¹H NMR (CDCl$_3$, 400 MHz)

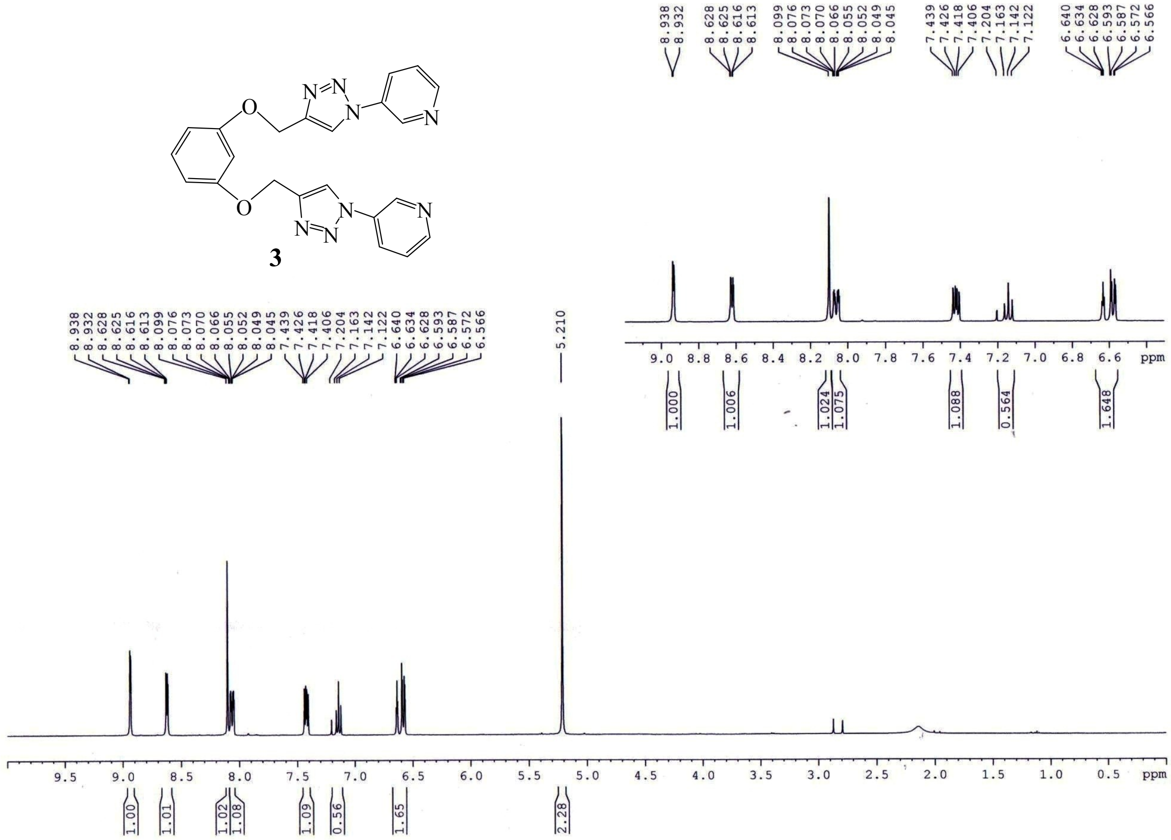

3

^{13}C NMR ($CDCl_3$, 100 MHz)

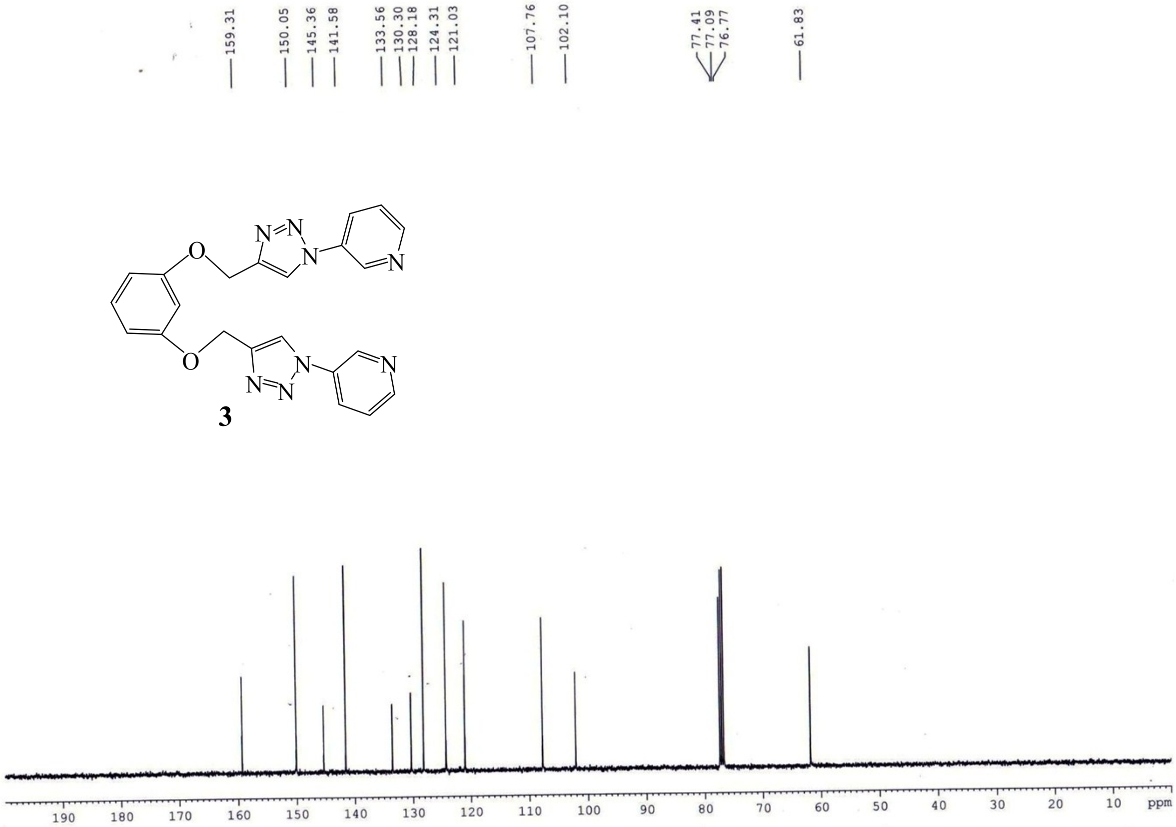

3

Mass spectrum of 3.

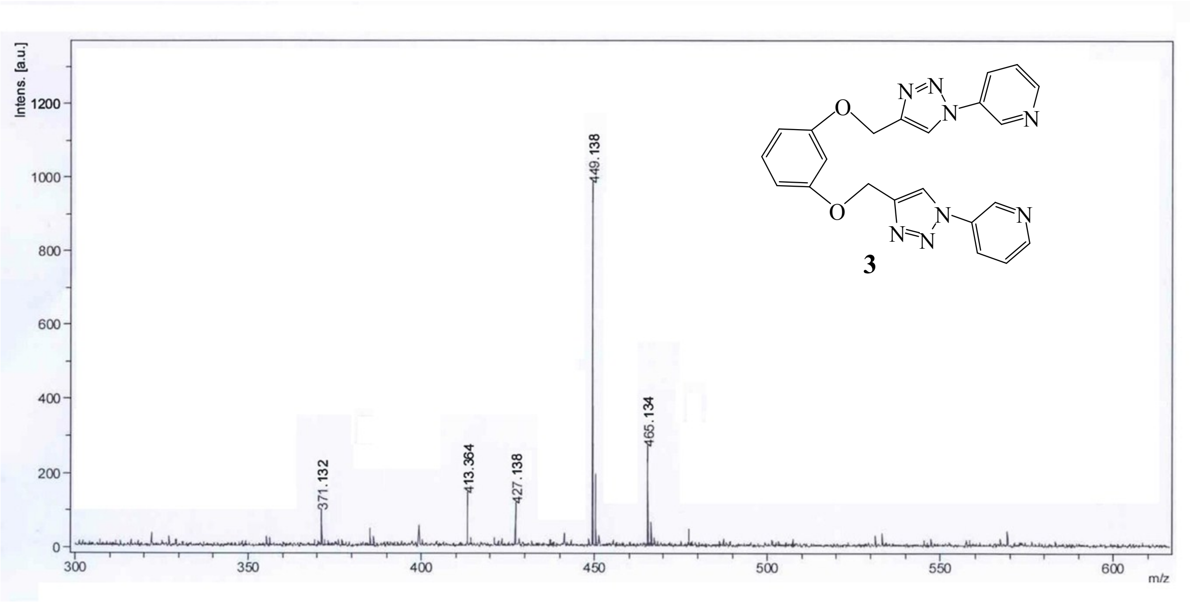

^{1}H NMR (d_6-DMSO, 400 MHz)

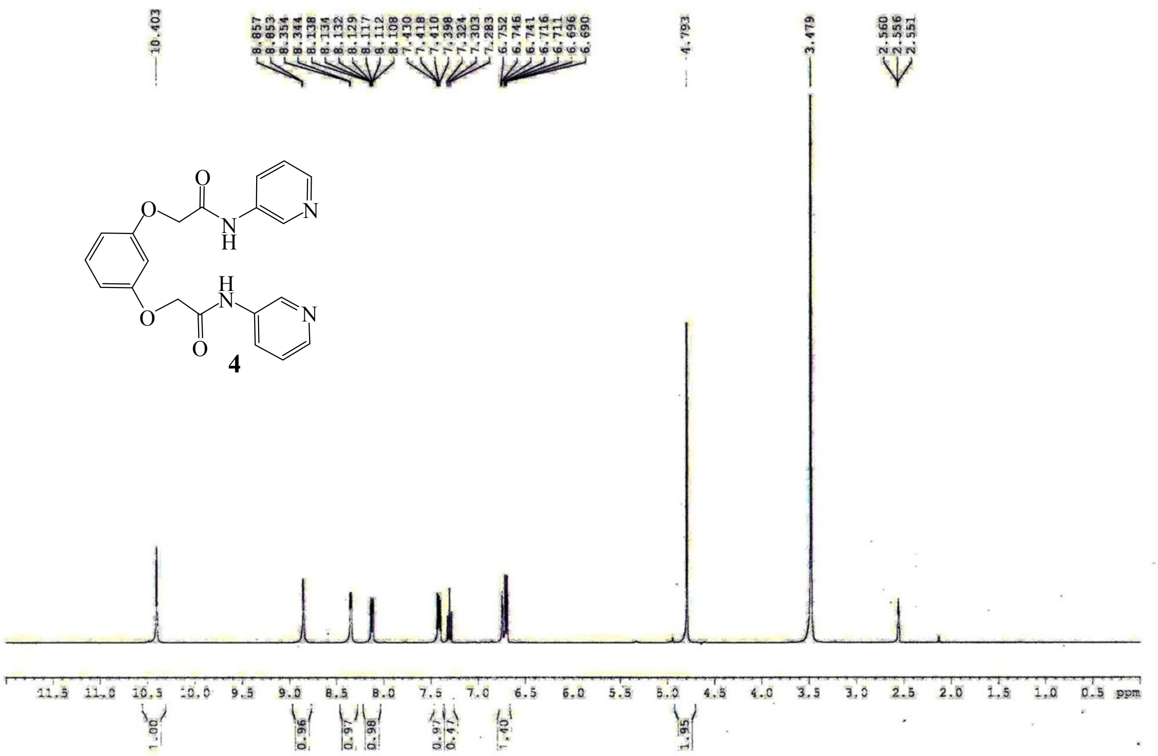

^{13}C NMR (*d$_6$*-DMSO, 100 MHz)

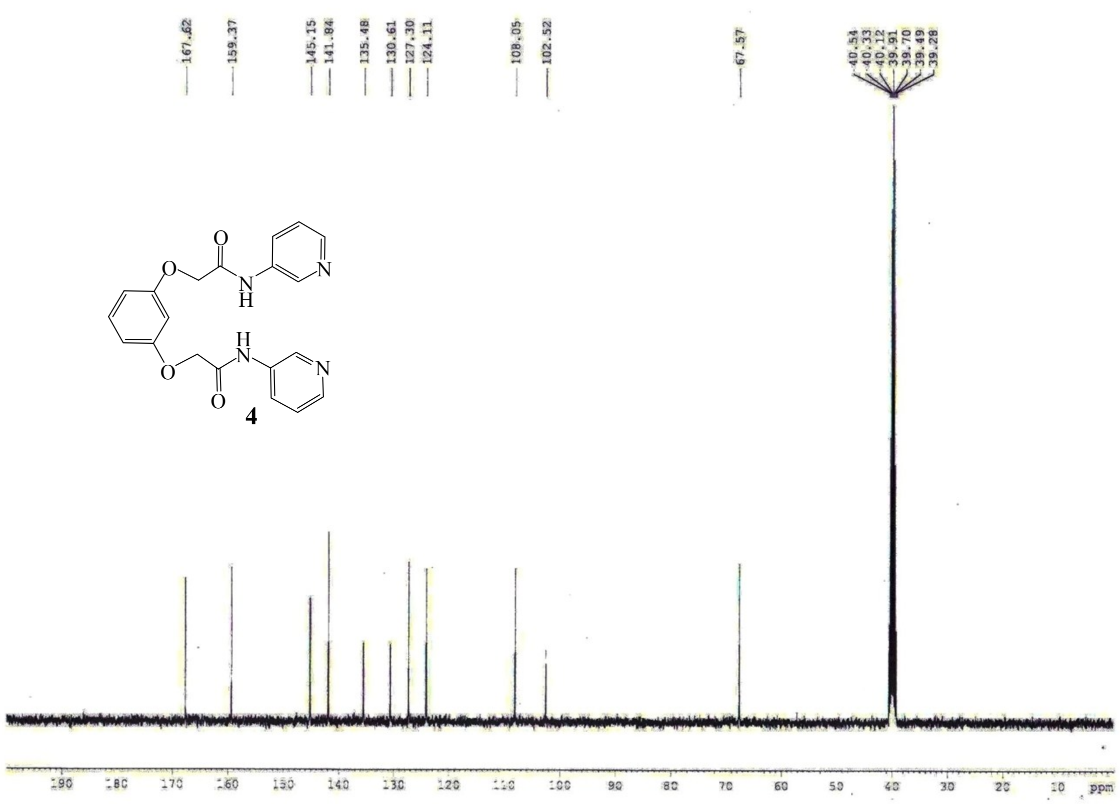

4

Mass spectrum of 4.